

## Supplementary Materials

### **A broadly neutralizing antibody against SARS-CoV-2 Omicron variant infection exhibiting a novel trimer dimer conformation in spike protein binding**

Yingdan Wang<sup>1#</sup>, Wuqiang Zhan<sup>1#</sup>, Jiangyan Liu<sup>1,2#</sup>, Yanqun Wang<sup>3#</sup>, Xiang Zhang<sup>1</sup>, Meng Zhang<sup>1</sup>, Lin Han<sup>1</sup>, Yunping Ma<sup>1</sup>, Lu Lu<sup>1</sup>, Yumei Wen<sup>1</sup>, Zhenguo Chen<sup>1</sup>, Jincun Zhao<sup>3,4\*</sup>, Fan Wu<sup>2\*</sup>, Lei Sun<sup>1\*</sup>, Jinghe Huang<sup>1\*</sup>

<sup>1</sup>Key Laboratory of Medical Molecular Virology (MOE/NHC/CAMS) and Shanghai Institute of Infectious Disease and Biosecurity, Shanghai Fifth People's Hospital, Shanghai Public Health Clinical Center, Institutes of Biomedical Sciences, School of Basic Medical Sciences, Fudan University, Shanghai, China.

<sup>2</sup>Shanghai Immune Therapy Institute, Shanghai Jiao Tong University School of Medicine Affiliated Renji Hospital, Shanghai, China.

<sup>3</sup>State Key Laboratory of Respiratory Disease, National Clinical Research Center for Respiratory Disease, Guangzhou Institute of Respiratory Health, the First Affiliated Hospital of Guangzhou Medical University, Guangzhou, Guangdong, China;

<sup>4</sup>Institute of Infectious Disease, Guangzhou Eighth People's Hospital of Guangzhou Medical University, Guangzhou, Guangdong, China.

#These authors contributed equally: Yingdan Wang, Wuqiang Zhan, Jiangyan Liu, Yanqun Wang

\*Correspondence: Jincun Zhao (zhaojincun@gird.cn) or Fan Wu (wufan@fudan.edu.cn) or Lei Sun (llsun@fudan.edu.cn) or Jinghe Huang (Jinghehuang@fudan.edu.cn)

**Keywords:** COVID-19; SARS-CoV-2; Neutralizing Ab; Omicron Variant

## 32 **Materials and Methods**

### 33 **Cell lines, proteins, plasmids, and participants**

34 HEK293T cells and Huh-7 cells were cultured in DMEM medium with 10% fetal  
35 bovine serum (FBS). HEK293F cells were cultured in SMM293 TII medium  
36 (Sino Biological). S Trimer and RBD proteins of SARS-CoV-2 and Omicron  
37 variant were purchased from Sino Biological. Spike genes of SARS-CoV-2<sup>1</sup>,  
38 Alpha, Beta, Gamma, Delta, and Omicron variants were synthesized and codon  
39 optimized by GenScript and constructed in pcDNA3.1 vector.  
40 Ethical approval was obtained from the Ethics Committee of the Shanghai  
41 Public Health Clinical Center for this study (YJ-2020-S021-01). All participants  
42 signed an informed consent approved by the Investigational Review Board  
43 (IRB).

### 44 **Memory B-cell staining, sorting and antibody cloning**

45 SARS-CoV-2-specific monoclonal antibodies were isolated from mononuclear  
46 cells (PBMC) of COVID-19 recovered patients by *in vitro* single B cells, as  
47 previously described<sup>2</sup>. We sorted CD19<sup>+</sup>IgA<sup>-</sup>IgD<sup>-</sup>IgM<sup>-</sup> memory B cells and plate  
48 them into 384-well plates in the presence of IL-21, IL-2, and feeder cells. After  
49 two weeks, supernatants were collected and screened for neutralization against  
50 SARS-CoV-2. Variable region of the heavy chain (VH) and the light chain (VL)  
51 of the immunoglobulin gene from wells with SARS-CoV-2 neutralization activity  
52 was amplified by RT-PCR. Antibodies were expressed by HEK293F cells and  
53 purified with protein G beads (Smart-Lifesciences).

### 54 **Expression and purification of SARS-CoV-2 Omicron Spike**

55 The Human codon gene encoding SARS-CoV-2 Omicron S ectodomain was  
56 purchased from GeneScript. The expression plasmid of Omicron S with  
57 HexaPro mutations<sup>3</sup> was constructed and transfected into suspension  
58 HEK293F using polyethlenimine. After 72 h, the supernatants were harvested  
59 and filtered for affinity purification by HisTrap HP (GE). The protein was then

60 further purified by gel filtration using Superose 6 increase 10/300 column (GE  
61 Healthcare) in 20 mM Tris pH 8.0, 200 mM NaCl.

### 62 **The preparation of Fab**

63 1 mg/mL papain (100 mM Tris, 2 mM EDTA, 1 mM DTT, pH8.0) was added into  
64 1 mg/mL IgG in 100 mM Tris, pH 8.0 by a mass ratio of 1:20 (papain:IgG). After  
65 two hours of incubation at 37.5 °C, papain was removed by ultrafiltration  
66 (Millipore), and Fc region was removed by Protein A/G Sepharose (SMART  
67 LIFESCIENCES).

### 68 **Production of Pseudoviruses**

69 Pseudoviruses were generated by co-transfection of 293T cells with a  
70 pcDNA3.1 expression plasmid encoding the respective spike protein and a  
71 pNL4-3.Luc.R-E- backbone<sup>4</sup>. Viral supernatant was collected after 48 h and  
72 frozen at -80 °C until use. Site-directed mutagenesis was used to construct 34  
73 Omicron single mutants and 20 single mutants involved in 6M6-RBD interaction.

### 74 **Neutralization assay**

75 Neutralization activities of mAbs were measured using a single-round  
76 pseudovirus infection of Huh-7 cells as previous described. MAbs were serially  
77 diluted with DMEM medium and incubated with 40 µL of pseudovirus at 37 °C  
78 for 1 h.  $1 \times 10^4$  Huh-7 cells were added to the mixture for infection. After 48 h,  
79 cells were lysed and luciferase activity were developed with a luciferase assay  
80 system (Promega). IC<sub>50</sub> was calculated as the concentration of mAb which  
81 results in a 50% reduction of relative luminescence units (RLU) compared with  
82 virus control.

### 83 **ELISA**

84 Trimer and RBD proteins of SARS-CoV-2 and Omicron variant (3 µg/mL) were  
85 coated on a MaxiSorp Nunc-immuno 96-well plate (Thermo Scientific, USA) at  
86 37 °C for 1.5 h and then blocked with 5% non-fat milk for 1 h at room  
87 temperature (RT). MAbs were serially diluted in disruption buffer (PBS, 2%

88 BSA, 5% FBS, and 1% Tween-20), added to the wells, and incubated for 1 h at  
89 RT. Horseradish peroxidase (HRP)-conjugated goat anti-human IgG antibody  
90 (Jackson Immuno Research Laboratories, USA) was added for 1 h at RT. Plates  
91 were washed, developed with ABST (Thermo Scientific, USA), and read at 405  
92 nm on a plate reader (Perkin Elmer, USA).

### 93 **Biolayer interferometry (BLI) binding assay**

94 Biolayer interferometry (FortéBio OctetRED96) was used to measure the  
95 kinetics of mAbs binding to RBD and S trimer proteins of SARS-COV-2 and  
96 Omicron variant. 10 µg/mL of mAb was immobilized on to anti-human IgG (AHC)  
97 biosensors, and then incubated with 6 µg/mL of RBD or S trimer protein. The  
98 assay followed sequential steps at 30°C as follows. (1) Equilibration with sterile  
99 water (60 s). (2) Immobilization of mAb onto sensors (200 s). (3) Baseline in  
100 kinetics buffer (PBS with 0.02% Tween) for 300 s. (4) Association of S trimer or  
101 RBD protein of SARS-CoV-2 or Omicron variant (300 s). (5) Dissociation of S  
102 trimer or RBD (0.02% PBST for 120 s). The buffer control binding was  
103 subtracted to deduct nonspecific binding.  $K_{on}$ ,  $K_{off}$ , and  $KD$  were calculated by  
104 FortéBio Data Analysis software (Version 8.1), using 1:1 binding and a global  
105 fitting model. Graph was generated using Graphpad Prism (GraphPad, San  
106 Diego, CA).

### 107 **Biolayer interferometry competition assay**

108 Ab cross-competition was conducted following the classical sandwich assay. 10  
109 µg/mL of S309 that immobilized on to anti-human IgG (AHC) biosensors was  
110 incubated with 6 µg/mL of RBD protein of SARS-COV-2 and then competed  
111 with 10 µg/mL of 6M6. (1) Baseline with sterile water for 60 s. (2) Immobilization  
112 of mAb S309 onto sensors (200 s). (3) Baseline in kinetics buffer (PBS with  
113 0.02% Tween) for 300 s. (4) Blocking biosensors with an IgG1 isotype control  
114 at 50 µg/mL (200 s). (5) Association of SARS-CoV-2 RBD (300 s). (6) Wash  
115 with 0.02% PBST for 120 s to reach baseline. (7) Competition: biosensors

116 immersed with 6M6 and at 10 µg/mL for 600 s to detect the association between  
117 mAb2 and SARS-CoV-2 RBD. REGN10989 was used as a negative control.

118 In ACE2 binding competition assay, biosensors were immobilized with 20  
119 µg/mL of ACE2-Fc for 600 s. Biosensors were then washed and incubated with  
120 the mixture of 600 nM of 6M6 and 100 nM SARS-CoV-2 RBD or Omicron S  
121 trimer for 600 s. An HIV-1 mAb VRC01 was used as an IgG1 isotype negative  
122 control. The mixture of VRC01 and SARS-CoV-2 RBD or Omicron S trimer was  
123 used as a positive control. Graph was generated using Graphpad Prism  
124 (GraphPad, San Diego, CA).

### 125 **Negative-stain electron microscopy**

126 Omicron S was mix with 6M6 IgG or Fab by a molar ratio of 1:1.5 or 1:3,  
127 respectively, then diluted to final 0.04 mg/mL and incubated for 10 min on ice.  
128 5µL of sample (Omicron S, Omicron S+6M6 IgG or Omicron S+6M6 Fab) was  
129 loaded to a glow-discharged carbon-coated copper grid (300 mesh,  
130 Zhongjingkeyi Technology) and incubated for 1 min. The excess sample liquid  
131 was removed with a filter paper and then the grid was stained with a droplet of  
132 2% uranyl acetate for 10s. The staining process was repeated three times.  
133 Finally, the excess staining buffer was removed, and the grid was dried at room  
134 temperature. The prepared grids were observed on a Talos L120C microscope  
135 (FEI) operating at 120 kV, using a Ceta2 camera (Thermo Fisher) at a nominal  
136 magnification of 120,000.

### 137 **Cryo-EM sample preparation**

138 Purified SARS-CoV-2 Omicron S at 1.554 mg/mL was mixed with 6M6 antibody  
139 by a molar ratio of 1:1.5, then diluted to final 0.5 mg/mL and incubated for 10  
140 min on ice before application onto a freshly glow-discharged holey amorphous  
141 nickel-titanium alloy film supported by 400 mesh gold grids<sup>5</sup> with microarray  
142 pattern similar like the commercial Quantifoil 1.2/1.3 grid. The sample was  
143 plunged freezing in liquid ethane using Vitrobot IV (FEI/Thermo Fisher

144 Scientific), with 2 s blot time and -3 blot force and 10 s wait time.

### 145 **Cryo-EM data collection and image processing**

146 Cryo-EM data were collected on a Titan Krios microscope (Thermo Fisher)  
147 operated at 300 kV, equipped with a K3 summit direct detector (Gatan) and a  
148 GIF quantum energy filter (Gatan) setting to a slit width of 20 eV. Automated  
149 data acquisition was carried out with SerialEM software<sup>6</sup> through beam-image  
150 shift method <sup>7</sup>.

151 Movies were taken in the super-resolution mode at a nominal magnification  
152 81,000 $\times$ , corresponding to a physical pixel size of 1.064 Å, and a defocus range  
153 from -1.2  $\mu\text{m}$  to -2.5  $\mu\text{m}$ . Each movie stack was dose-fractionated to 40 frames  
154 with a total exposure dose of about 58 e-/Å<sup>2</sup> and exposure time of 3s.

155 All the data processing was carried out using either modules on, or through,  
156 RELION v3.0<sup>8</sup> and cryoSPARC <sup>9</sup>. A total of 3,848 movie stacks was binned  
157 2  $\times$  2, dose weighted, and motion corrected using MotionCor2<sup>10</sup> within RELION.  
158 Parameters of contrast transfer function (CTF) were estimated by using Gctf<sup>11</sup>.  
159 All micrographs then were manually selected for further particle picking upon  
160 ice condition, defocus range and estimated resolution.

161 Remaining 3,027 good images were imported into cryoSPARC for further  
162 patched CTF-estimating, blob-picking and 2D classification. From 2D  
163 classification, trimer dimer and trimer particles were observed. Several good 2D  
164 classes of these two kind particles were used as templates for template-picking  
165 separately. After 2D classification of particles from template-picking was  
166 finished, all good particles from blob-picking and template-picking were merged  
167 and deduplicated, subsequently being exported back to RELION through pyem  
168 package<sup>12</sup>.

169 For trimer dimer map, 787,342 particles were extracted at a box-size of 480 and  
170 rescaled to 160 (Supplementary information, **Table. S1**), then carried on 2  
171 round of 3D classification with a soft circular mask of 400 Å in diameter in  
172 RELION. Only good classes were selected, yielding 166,441 clean particles.

173 These particles were re-extracted unbinned (1.064 Å/pixel) and auto-refined  
174 without applying symmetry, then CTF-refined and polished, yielding a map at  
175 3.76 Å. This map showed a relatively symmetrical structure with all six RBDs  
176 up and each RBD combined a Fab. So, we further ran auto-refinement by  
177 applying C3 symmetry and got a 3.45 Å map. The density of omicron spike was  
178 improved in the map, but the interfaces from RBD with Fab and from Fab with  
179 another Fab were still not clear enough. To solve this, we expanded the  
180 particles with C3 symmetry and subtracted the signal with a mask consist of a  
181 pair of RBDs and Fabs, then carried on local 3D-classification with the same  
182 mask. In final, 134,249 particles yielded a 3.32 Å local map after local auto-  
183 refinement.

184 For trimer map, 787,342 particles were extracted at a box-size of 320 and  
185 rescaled to 160, then carried on 2 round of 3D classification with a soft circular  
186 mask of 220 Å in diameter in RELION. Only good classes were selected,  
187 yielding 399,010 clean particles. These particles were re-extracted unbinned  
188 (1.064 Å/pixel) and auto-refined, then CTF-refined and polished, yielding a map  
189 at 3.10 Å. This map showed two RBDs up and each up RBD combined a partial  
190 Fab due to flexibility. To resolve more density, we did local 3D-classification  
191 with the mask of one better RBD and its combined Fab. Finally, 272,354  
192 particles were auto-refined entirely and yielding an overall 3.18 Å resolution  
193 map.

194 The reported resolutions above are based on the gold-standard Fourier shell  
195 correlation (FSC) 0.143 criterion. All the visualization and evaluation of 3D  
196 density maps were performed with UCSF Chimera<sup>13</sup>. The above procedures of  
197 data processing are summarized in Fig.S2. These sharpened maps were  
198 generated by DeepEMhancer<sup>14</sup> and then “vop zflip” to get the correct  
199 handedness in UCSF Chimera for subsequent model building and analysis.

## 200 **Model building and refinement**

201 For model building of SARS-CoV-2 Omicron S-6M6 complex, the SARS-CoV-

202 2 Omicron S trimer model and the antibody model generated by swiss-model  
203 were fitted into the map using UCSF Chimera and then manually adjusted with  
204 COOT<sup>15</sup>. Several iterative rounds of real-space refinement were further carried  
205 out in PHENIX<sup>16</sup>. The two opposite RBDs domain bound with two antibodies  
206 was refined against the local refinement map and then docked back into the  
207 into global refinement trimer and trimer dimer maps. Model validation was  
208 performed using MolProbity. Figures were prepared using UCSF Chimera and  
209 UCSF ChimeraX.

210

## 211 REFERENCES

- 212 1 Wu, F. *et al.* A new coronavirus associated with human respiratory disease in China. *Nature*  
213 **579**, 265-269, doi:10.1038/s41586-020-2008-3 (2020).
- 214 2 Huang, J. *et al.* Isolation of human monoclonal antibodies from peripheral blood B cells.  
215 *Nat Protoc* **8**, 1907-1915, doi:10.1038/nprot.2013.117 (2013).
- 216 3 Hsieh, C. L. *et al.* Structure-based design of prefusion-stabilized SARS-CoV-2 spikes.  
217 *Science* **369**, 1501-1505, doi:10.1126/science.abd0826 (2020).
- 218 4 Wu, F. *et al.* Evaluating the Association of Clinical Characteristics With Neutralizing  
219 Antibody Levels in Patients Who Have Recovered From Mild COVID-19 in Shanghai, China.  
220 *JAMA Intern Med*, doi:10.1001/jamainternmed.2020.4616 (2020).
- 221 5 Huang, X. *et al.* Amorphous nickel titanium alloy film: A new choice for cryo electron  
222 microscopy sample preparation. *Prog Biophys Mol Biol* **156**, 3-13,  
223 doi:10.1016/j.pbiomolbio.2020.07.009 (2020).
- 224 6 Mastronarde, D. N. Automated electron microscope tomography using robust prediction  
225 of specimen movements. *J Struct Biol* **152**, 36-51, doi:10.1016/j.jsb.2005.07.007 (2005).
- 226 7 Wu, C., Huang, X., Cheng, J., Zhu, D. & Zhang, X. High-quality, high-throughput cryo-  
227 electron microscopy data collection via beam tilt and astigmatism-free beam-image shift.  
228 *J Struct Biol* **208**, 107396, doi:10.1016/j.jsb.2019.09.013 (2019).
- 229 8 Zivanov, J. *et al.* New tools for automated high-resolution cryo-EM structure  
230 determination in RELION-3. *Elife* **7**, doi:10.7554/eLife.42166 (2018).
- 231 9 Punjani, A., Rubinstein, J. L., Fleet, D. J. & Brubaker, M. A. cryoSPARC: algorithms for rapid  
232 unsupervised cryo-EM structure determination. *Nat Methods* **14**, 290-296,  
233 doi:10.1038/nmeth.4169 (2017).
- 234 10 Zheng, S. Q. *et al.* MotionCor2: anisotropic correction of beam-induced motion for  
235 improved cryo-electron microscopy. *Nat Methods* **14**, 331-332, doi:10.1038/nmeth.4193  
236 (2017).
- 237 11 Zhang, K. Gctf: Real-time CTF determination and correction. *J Struct Biol* **193**, 1-12,  
238 doi:10.1016/j.jsb.2015.11.003 (2016).
- 239 12 Asarnow, D., Palovcak, E., Cheng, Y. UCSF pyem v0.5. Zenodo



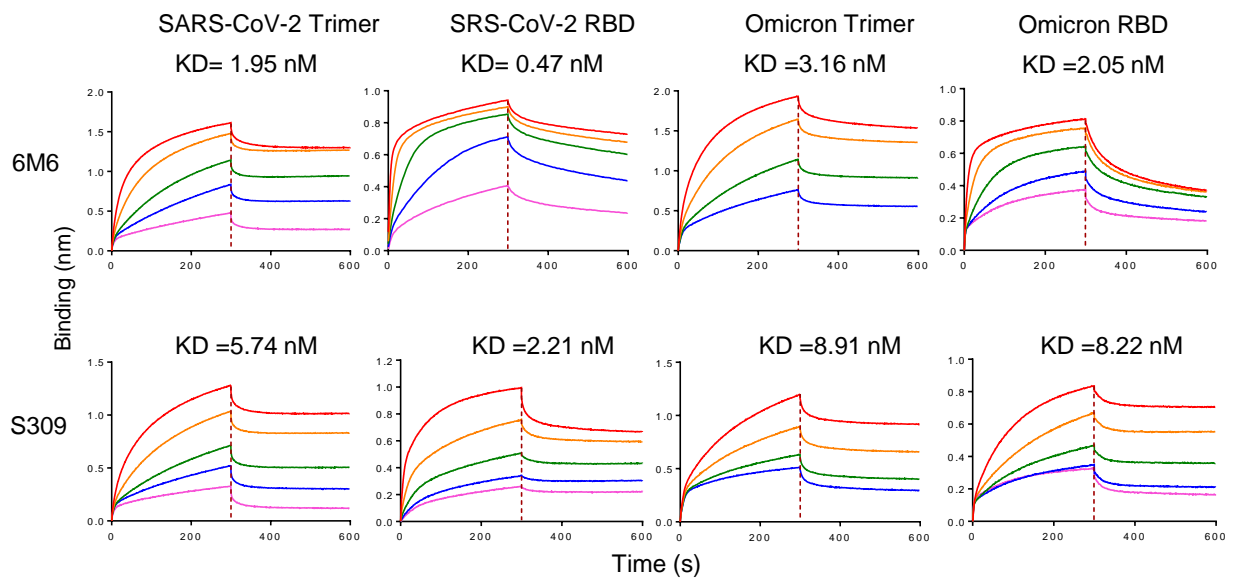
240 <https://doi.org/10.5281/zenodo.3576630> (2019).  
241 [doi:https://doi.org/10.5281/zenodo.3576630](https://doi.org/10.5281/zenodo.3576630)  
242 13 Pettersen, E. F. *et al.* UCSF Chimera--a visualization system for exploratory research and  
243 analysis. *J Comput Chem* **25**, 1605-1612, doi:10.1002/jcc.20084 (2004).  
244 14 Sanchez-Garcia, R. *et al.* DeepEMhancer: a deep learning solution for cryo-EM volume  
245 post-processing. *Commun Biol* **4**, 874, doi:10.1038/s42003-021-02399-1 (2021).  
246 15 Emsley, P., Lohkamp, B., Scott, W. G. & Cowtan, K. Features and development of Coot.  
247 *Acta Crystallogr D Biol Crystallogr* **66**, 486-501, doi:10.1107/S0907444910007493 (2010).  
248 16 Afonine, P. V. *et al.* Real-space refinement in PHENIX for cryo-EM and crystallography.  
249 *Acta Crystallogr D Struct Biol* **74**, 531-544, doi:10.1107/S2059798318006551 (2018).  
250  
251  
252

253  
254

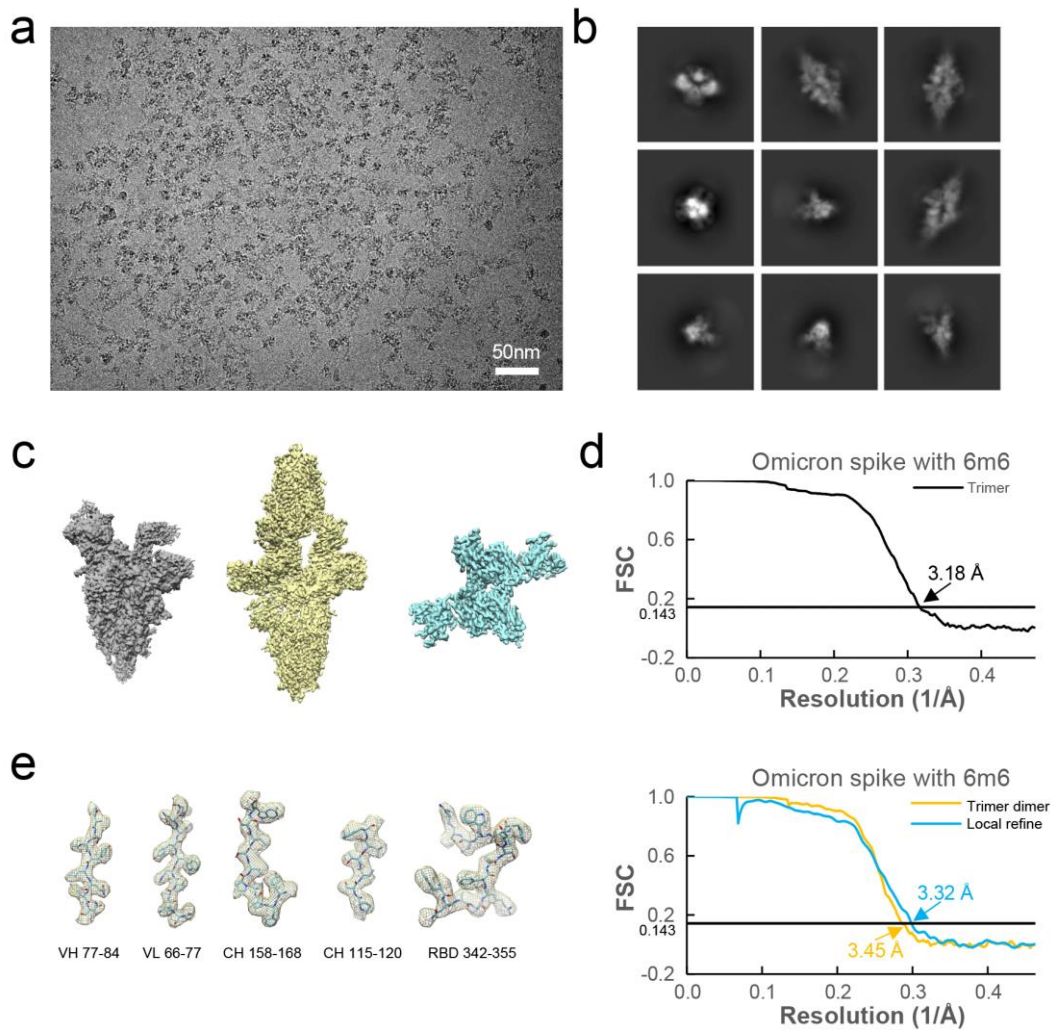
**Supplementary Table S1. Cryo-EM data collection and refinement statistics.**

	Trimer (EMD-32552) (PDB 7WJY)	Trimer dimer (EMD-32553) (PDB 7WJZ)	RBD-6M6 local (EMD-32554) (PDB 7WK0)
<b>Data collection and processing</b>			
Magnification		81,000	
Voltage (kV)		300	
Electron exposure (e-/Å <sup>2</sup> )		58	
Defocus range (µm)		-1.2 to -2.5	
Pixel size (Å)		1.064	
Pixel size (Å)		787,342	
Initial particles (no.)			
Symmetry imposed	C1	C3	C1
Final particles (no.)	272,354	166,441	134,249
Map resolution (Å)	3.18	3.45	3.32
<b>Refinement</b>			
R.m.s. deviations	0.003	0.002	0.004
Bond lengths (Å)	0.669	0.506	0.640
Bond angles (°)			
Validation			
MolProbity score	2.58	2.50	2.78
ClashscoreRotamers	8.37	8.10	9.33
outliers (%)	6.81	5.33	7.71
Ramachandran plot			
Favored (%)	91.73	91.52	87.54
Allowed (%)	8.05	8.45	12.30
Disallowed (%)	0.22	0.03	0.16

255  
256



257 **Supplementary Fig. S1. The binding affinity of 6M6 to the S trimer and**  
 258 **RBD of SARS-CoV-2 and the Omicron variant. S309 was used as a control.**



259

260 **Supplementary Fig. S2. Cryo-EM data collection and processing of 6M6-**

261 **bound SARS-CoV-2 Omicron S. (a) Representative electron micrograph. (b)**

262 **2D classification results of 6M6-bound SARS-CoV-2 S. (c) The reconstruction**

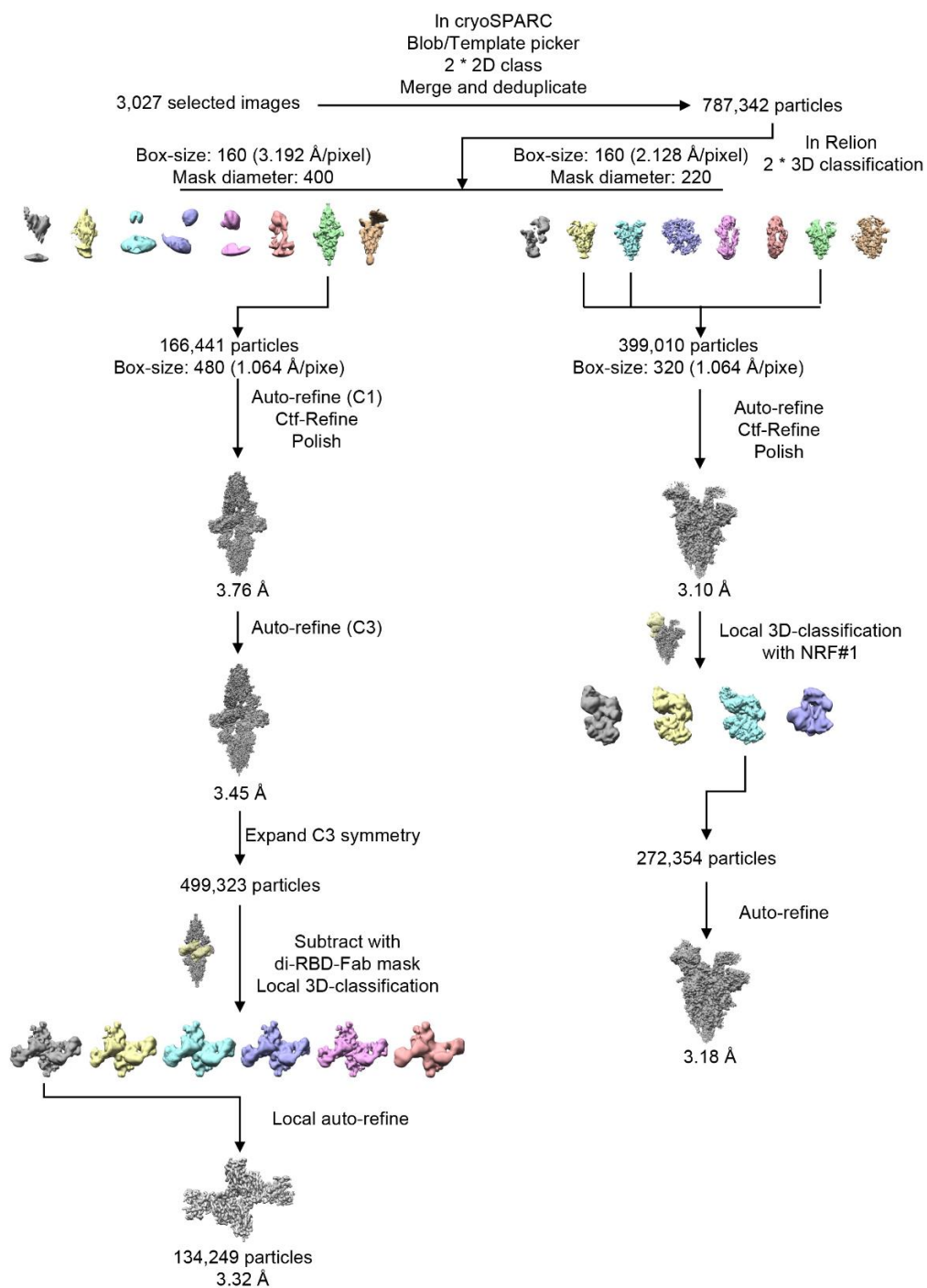
263 **map of the complex structures in two states and one local refinement map. (d)**

264 **Gold-standard Fourier shell correlation curves for each structure. The 0.143**

265 **cutoff is indicated by a horizontal dashed line. (e) Representative high-**

266 **resolution density of different domains in the local refined map.**

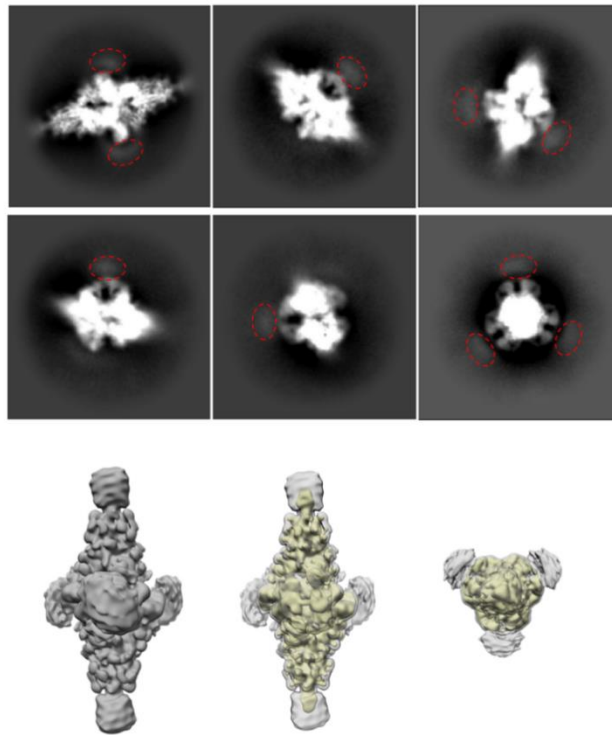
Omicron S-6m6



267

268 **Supplementary Fig. S3. Data processing flowchart of the 6M6-bound**

269 **SARS-CoV-2 Omicron S trimer.**

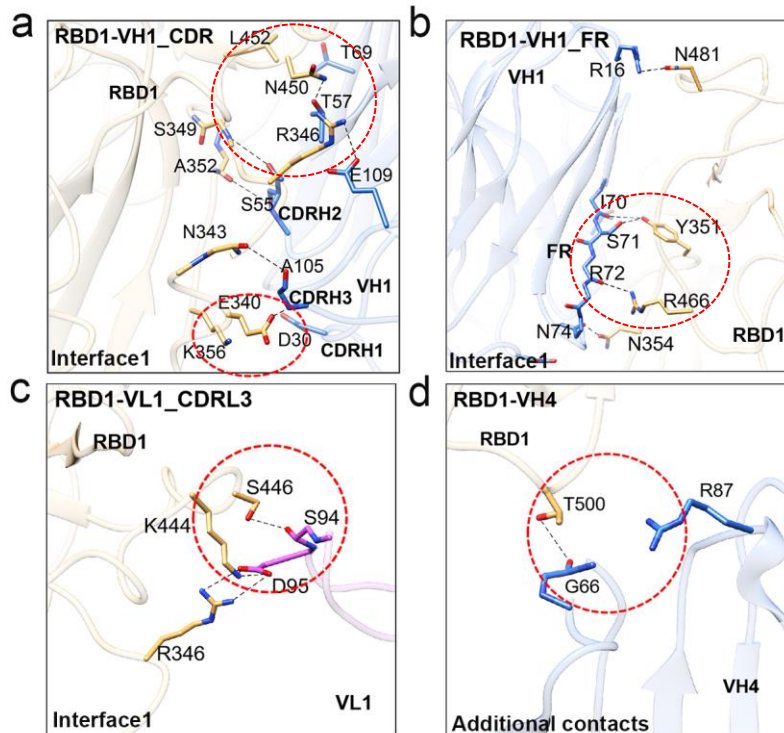


270 **Supplementary Fig. S4. Fc domains of IgGs indicated in cryo-EM data.**

271 Vague density of Fc domains in 2D classification and 3D-refined map (low-

272 passed to 15 Å) of trimer dimer. The gray map is at the low range level in

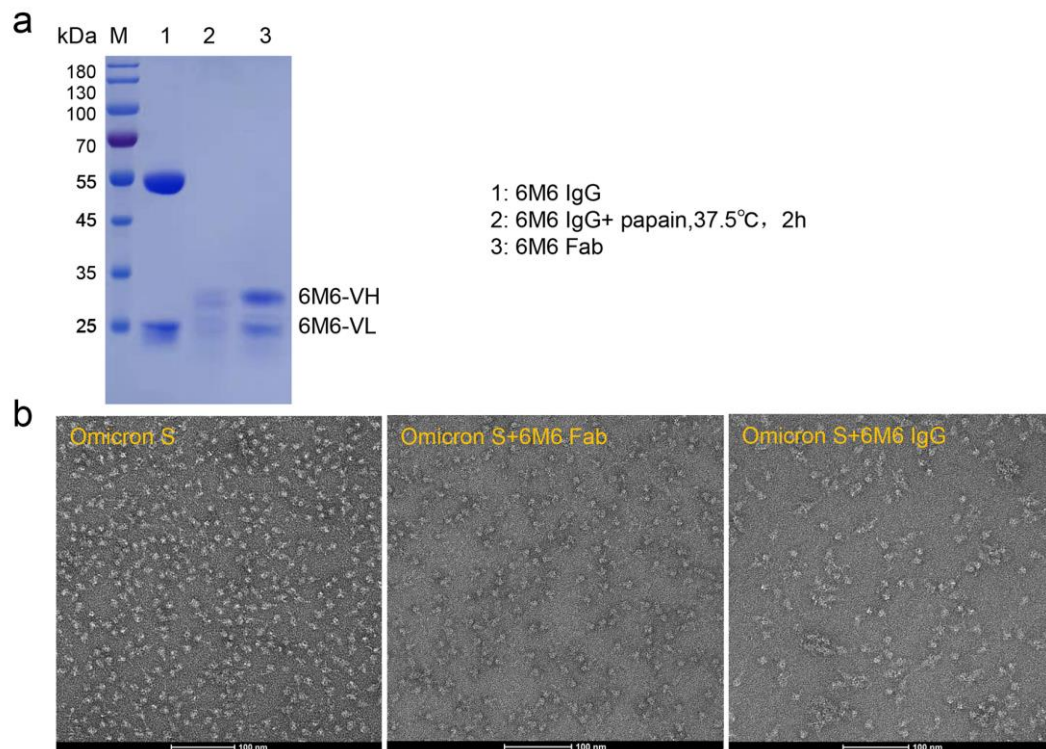
273 Chimera, and the yellow map is at the normal range level.



274

275

276 **Supplementary Fig. S5. The interaction between RBD1 and 6M6.** The  
 277 detailed interactions between Omicron S RBD1 and 6M6 VH1 CDR **(a)**, FR **(b)**,  
 278 or VL1 CDRL3 **(c)**. The interaction between 6M6 and RBD1 was slightly  
 279 different from the interaction between 6M6 and RBD4. The salt bridge between  
 280 K356 from RBD4 and D30 of CDRH1 was not formed between 6M6 and RBD1  
 281 **(a)**. As a compensation, S446 of RBD1 is closer to VL1 and forms an extra  
 282 hydrogen bond **(c)**. The residues participating in interactions are represented  
 283 as sticks. Polar interactions are indicated as dotted lines. **(d)** The additional  
 284 interaction between Omicron S RBD1 and 6M6 VH4 in trimer dimer (interface  
 285 2). The interface 2 of RBD1 bears only one hydrogen bond between T500 of  
 286 RBD1 and G66 of VH4. The residues involved in different interactions are  
 287 enclosed in red dotted circles.

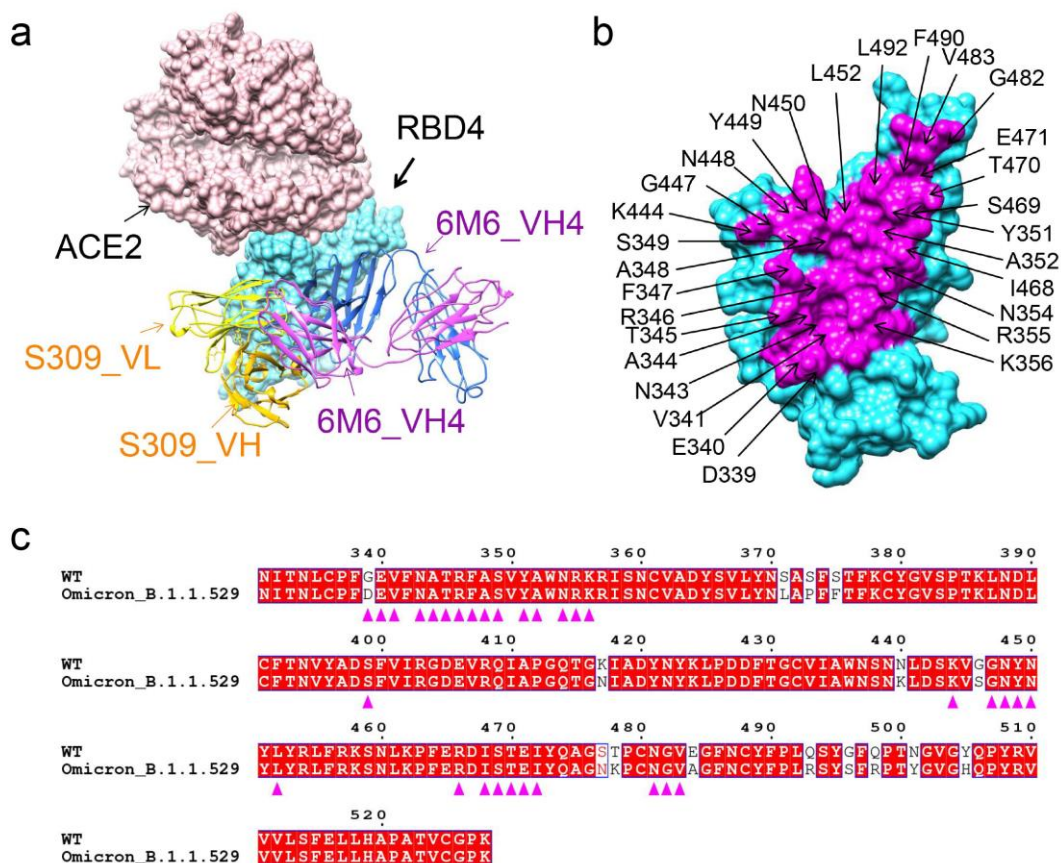


288

289 **Supplementary Fig. S6. IgG 6M6 crosslinks Omicron S trimers to form**  
 290 **trimer dimer. (a) SDS-PAGE of the 6M6 in IgG and fab form. (b) Negative**  
 291 **stain images of Omicron S trimer-6M6 Fab and Omicron S trimer-6M6 IgG,**  
 292 **showing that only 6M6 IgG can induce the formation of trimer dimer.**

293





294

295 **Supplementary Fig. S7. The epitope of 6M6 on Omicron RBD. (a)** 6M6

296 engages an epitope outside of RBM and does not clash with ACE2. Ribbon

297 diagrams of 6M6, S309 (PDBID: 6WPS) and ACE2 (PDBID: 7T9L) bound to the

298 Omicron S RBD. **(b)** Close-up view of 6M6 epitope. The residues involved in

299 the interaction are labeled. **(c)** Sequence alignment of RBD region of SARS-

300 CoV-2 WT and Omicron. The strictly conserved amino acid residues are

301 highlighted in red. Purple triangles point out the amino acid residues on the

302 RBD involved in the major interactions for 6M6.

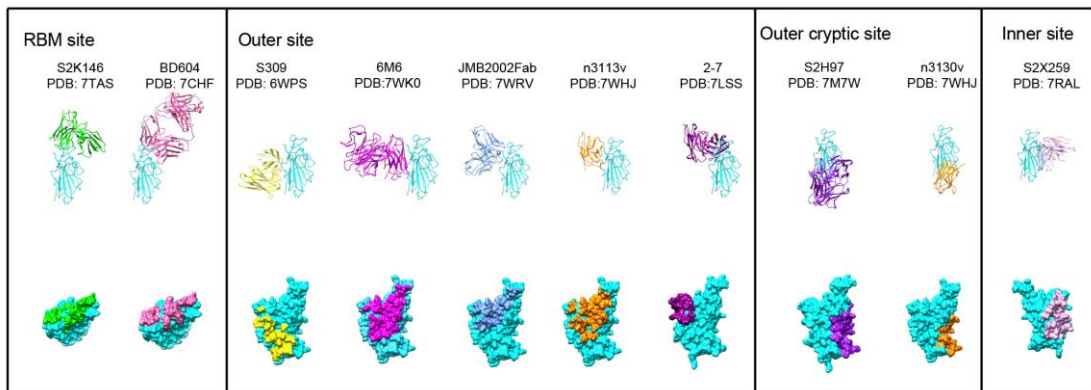
303

304

305

306

307



309

310

311

312

313

314

315

**Supplementary Fig. S8. Epitope classification of broadly neutralizing antibodies against all six of SARS-CoV-2 VOCs.** The SARS-CoV-2 RBD (cyan) is shown in the same relative orientation in the ribbon model, antibodies are colored differently. The SARS-CoV-2 RBD is shown in cyan surface, the epitopes of antibodies are colored by their model.